JOURNAL OF Materials CHEMISTRY

Preparation of fine single crystals of spinel-type lithium manganese oxide by LiCl flux method for rechargeable lithium batteries. Part 1. $LiMn_2O_4$

Weiping Tang,[a] Xiaojing Yang,[b] Zhonghui Liu,[b] Shuji Kasaishi[b] and Kenta Ooi[b]

[a]*Research Institute for Solvothermal Technology, 2217-43, Hayashi-cho Takamatsu 761-0301, Japan*
[b]*Marine Resources and Environment Research Institute, National Institue of Advanced Industrial Science and Technology, 2217-14, Hayashi-cho Takamatsu 761-0395, Japan*

Received 2nd April 2002, Accepted 9th July 2002
First published as an Advance Article on the web 23rd August 2002

Uniform fine single crystals of $LiMn_2O_4$ spinel were synthesized by a LiCl–$Mn(NO_3)_2$ flux method. The effects of reaction temperature and time on the composition, size and morphology of lithium manganese oxide were investigated by chemical, X-ray diffraction and selected area electron diffraction analyses, and SEM observation. The composition and size of the single crystals depended strongly on the heating temperature. Stoichiometric $LiMn_2O_4$ single crystals were yielded at 850 °C, whereas lithium-rich and lithium-poor crystals were obtained at 650–750 °C and 950 °C, respectively. Plate-like $Li_{1.18}Mn_2O_{4.28}$ single crystals with a thickness of less than 0.1 μm, showed a high first discharge capacity of 112 mAh g^{-1} with a good cycle feature. The increase in the size of single crystals resulted in a decrease of the capacity at the first cycle, but did not accelerate the capacity fade over the following cycles.

Introduction

The spinel-type lithium manganese oxide, $LiMn_2O_4$ is an attractive cathode material for advanced lithium rechargeable batteries because of its cost, performance and non-toxicity.[1,2] The cathodic reaction in $LiMn_2O_4$ during the charge/discharge process proceeds with a lithium ion diffusion process moving from one 8a tetrahedron into another 8a site *via* an energetically unfavorable neighboring 16c octahedron in the crystal lattice.[3] A single crystal of $LiMn_2O_4$ containing a continuous lattice structure is more advantageous to the lithium diffusion process than a polycrystal which contains energy barriers in the form of grain boundaries. On the other hand, a single crystal $LiMn_2O_4$ has been reported as having a lithium ion diffusion coefficient of 10^{-11} S cm^{-2}, an order of magnitude lower than that of polycrystalline $LiMn_2O_4$.[4–7] This disadvantage, however, can be overcome by controlling the size of the single crystals. Therefore, fine single crystals of $LiMn_2O_4$ are probably better suited for practical use as a cathode material.

The spinel-type lithium manganese oxides are commonly prepared *via* a solid-state reaction,[8–11] which requires heating for a long time and results in non-homogeneous polycrystals with irregular morphology and broad particle-size distribution. To overcome these disadvantages, several solution routes have been developed, such as hydrothermal reaction,[12,13] sol–gel process,[14,15] co-precipitation,[16] and pechini process.[17] These methods require difficult conditions of high pressure or/and a large quantity of solvent and organic materials like citric acid, ethylene glycol, poly(vinyl alcohol). Moreover, because the final products obtained need firing to promote crystallinity, these methods generally give a polycrystalline powder of $LiMn_2O_4$. As far as we know, preparation of fine single crystals of $LiMn_2O_4$ has not been reported.

Recently, we have developed a ''Li-containing flux method'' to prepare lithium manganese oxides.[18–24] Since the rates of element diffusion in the salt melt are much higher than those in the solid-state, this method accelerates the formation reaction to give homogeneous manganese oxide compounds with regular morphology and narrow-size distribution. The lithium process can be classified into two categories: 1, dissolution–recrystallization; and 2, intercalation into manganese oxide precursor. The dissolution–recrystallization process proceeds in LiCl, LiOH melts or in $Li(NO_3)_2$, $LiCO_3$ melts at high temperature to form single crystals or manganese oxide crystals with a particular shape and distinguishable crystal plane and edge. We obtained $LiMnO_2$ and Li_2MnO_3 single crystals by use of a LiCl–MnOOH flux system,[18–29] and $LiMn_2O_4$ crystals by a LiCl–$MnCl_2$ flux evaporation system.[21] The intercalation reaction takes place in melts at low temperature while maintaining the size and shape of the particles of the precursors. By using a $LiNO_3$ melt lower than 400 °C, spinel-type lithium manganese oxides were produced by lithium diffusion to manganese oxide precursors such as γ-MnOOH, β-MnO_2 and birnessite.[23–25]

In this study, we report the preparation of fine single crystals of $LiMn_2O_4$ using the LiCl–$Mn(NO_3)_2$ flux system. Because LiCl is a neutral salt, it was expected to have high solubility for manganese and stabilize Mn^{3+} in the LiCl melt,[19,30] in contrast to salts containing oxygen.[22,23] The LiCl–$Mn(NO_3)_2$ flux system has an additional advantage in that $Mn(NO_3)_2$ is more reactive than solid manganese oxide.

Experimental

Preparation of single crystal $LiMn_2O_4$

Single crystals of $LiMn_2O_4$ were prepared from a LiCl–$Mn(NO_3)_2$ system in which LiCl was used as the flux and lithium source and $Mn(NO_3)_2$ as the manganese source. To obtain a uniform mixture of lithium and manganese sources, a $Mn(NO_3)_2$ solution (10.6 g) with 38 wt.% concentration was added to 50 g of LiCl. The weight ratio of $Mn(NO_3)_2$ to LiCl was 0.08 (mole ratio = 0.02). The mixture was dried at 120 °C for 4 h and put into an alumina crucible. The crucible was heated in an electric furnace to a range of 650–950 °C for 4 min. The electric furnace was then allowed to cool to room temperature naturally. The cooling progresses exponentially, and it took 10 and 60 min to lower the temperature from

650 and 950 °C to 610 °C (melting point of LiCl), respectively. The single crystals of $LiMn_2O_4$ were obtained after the melt was dissolved and washed in distilled water, filtered and dried at 100 °C. The samples are abbreviated as 650-4m, 750-4m, 850-4m and 950-4m respectively, where the former numbers correspond to the temperature and the latter numbers and letter the duration of maintenance at that temperature.

The effect of heating time on size and shape of single crystals was investigated. The $LiMn_2O_4$ formation reaction in the LiCl–$Mn(NO_3)_2$ flux was carried out at 650 °C and 750 °C for 2, 8 and 24 h, respectively. The products obtained at 650 °C and 750 °C were abbreviated as 650-2h, 650-8h and 650-24h, and 750-2h, 750-8h and 750-24h.

Post-annealing was carried out for 650-4m, 750-4m, 850-4m and 950-4m at 750 °C for 4 h to promote their crystallinity. The samples after post-annealing are abbreviated as A650-4m, A750-4m, A850-4m and A950-4m.

Physical analysis

X-Ray diffraction (XRD) analyses were carried out using a Rigaku type RINT1200 X-ray diffractometer with a graphite monochrometer. The lattice distance was calculated from d values corresponding to (3 1 1), (2 2 2), (4 0 0) (3 3 1) and (5 1 1) crystal planes by use of the RIGAKU lattice distance precision program. Scanning electron microscopy (SEM) was carried out on a JEOL type JSM-5310 scanning electron microscope. The selected area electron diffraction (SAED) analysis was carried out on a JEOL type JEM-3010 transmission electron microscope. DTA-TG curves were obtained on a Shimadzu type (DTG-50) thermal analyzer at a heating rate of 10 K min^{-1} in air.

Chemical analysis

Lithium and manganese contents of the crystals were determined by atomic absorption spectrometry after dissolving them in a mixed solution of HCl and H_2O_2. A mixed solution of HNO_3 and H_2O_2 in which the crystals were dissolved was used for detection of chloride by the addition of a $AgNO_3$ solution. No chloride was detected in the crystals. The available oxygen of each sample was determined by the standard oxalic acid method. The mean oxidation number of manganese (Z_{Mn}) and oxygen content were calculated from the value of available oxygen.[26]

Electrochemical measurement

The electrochemical cell used was Li/$LiPF_6$ in DEC-EC/single crystals of $LiMn_2O_4$. A mixture of the single crystals of $LiMn_2O_4$ (75 wt.%), acetylene black (17.5 wt.%), and Teflon binder (7.5 wt.%) was used as a cathode. The cathode mixture was pasted onto an aluminium foil. A disc shaped cathode with 2 cm^2 in area was then cut out after drying and pressing. A lithium sheet was used as the anode, a polypropylene non-woven cloth as a separator, and a DEC-EC (1 : 1 by weight) solution containing 1 mol dm^{-3} $LiPF_6$, as the electrolyte. The cell reaction was repeated in the potential range of 3–4.3 V with a constant current density of 0.2 mA cm^{-2} at 25 °C.

Results and discussion

Reaction in the LiCl–$Mn(NO_3)_2$ flux

The thermal behavior in the LiCl–$Mn(NO_3)_2$ flux system was studied by TG-DTA analysis (Fig. 1). The DTA curve shows four endothermic peaks at 91, 149, 240 and 610 °C. Weight losses of 1.6% and 1.5% around 91 and 149 °C, and 5.3% and 1.2% around 330 and 430 °C are found in the TG curve, respectively. To identify these peaks and weight losses, the mixture was heated to 200, 300, 400 and 500 °C. After the heating, the mixture was immersed in water and the precipitates

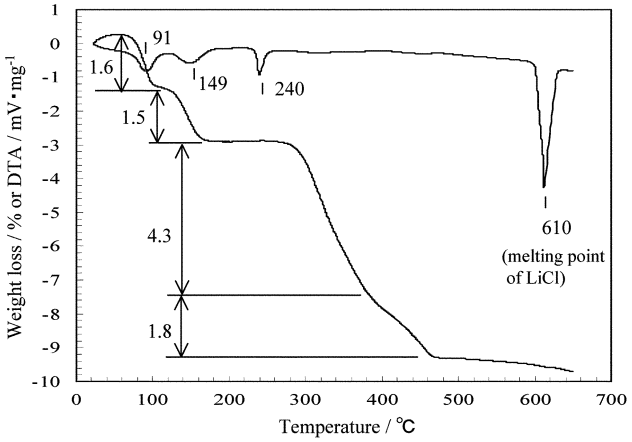

Fig. 1 TG-DTA curve of the LiCl–$Mn(NO_3)_2$ flux system.

were filtered. No reaction product was found at 200 °C, while black products were obtained above 300 °C. XRD analysis of the products obtained at 300 and 400 °C indicates that they were crystalline, which gives diffraction main peaks at 2θ = 19.5, 11.8 and 35.7°. The patterns differ from those obtained by the decomposition of $Mn(NO_3)_2$ in air (mainly β-MnO_2 or γ-MnO_2).[27–29] Chemical analyses show both the products contain 60% and 59% of manganese element, respectively, and less than 0.1% of lithium element each. Since the manganese contents are nearly equal to that of MnO_2 (63%), the products may be a mixture of different types of manganese dioxides. A single phase of spinel-type manganese oxides was formed at 500 °C. The two peaks at 91 °C and 149 °C with weight losses can be ascribed to the dehydration of the mixture. The peak at 240 °C and the weight loss around 330 °C is identified as the formation of manganese oxides by decomposition of $Mn(NO_3)_2$, and the weight loss around 430 °C as the formation reaction of spinel lithium manganese oxide. The above results suggest that the formation reaction of $LiMn_2O_4$ proceeds in two steps: 1, the decomposition of $Mn(NO_3)_2$ to form manganese dioxides; and 2, the formation of spinel lithium manganese oxide by reaction between the manganese oxide precursor and LiCl. The hypothetical formation reaction of $LiMn_2O_4$ can be written as:

$$2LiCl + 4Mn(NO_3)_2 = 2LiMn_2O_4 + 8NO_2 + Cl_2 \quad (1)$$

The theoretical weight loss of reaction (1) can be calculated as 54%. Since the weight ratio of $Mn(NO_3)_2$ to LiCl is 0.08 in the starting mixture, the weight loss of the mixture can be calculated as 4.6% for reaction (1). The weight loss (6.1%) between 300 and 500 °C in the TG curve agreed comparatively well with the calculated value. A slight difference in the weight loss may be due to the evaporation of small amount of metal salt.

Reaction (1) shows that spinel lithium manganese oxide forms with oxidation of Cl^- ions in the molten LiCl. The oxidation of Cl^- ions was reported in the creation of Li_2MnO_3 crystals with a LiCl–MnOOH flux system, and $LiMn_2O_4$ crystals by a LiCl–$MnCl_2$ flux system with a fixed Li : Mn molar ratio.[20,21] In these systems, because manganese sources contain Mn^{3+} and Mn^{2+}, the oxidation of Cl^- ions proceeds mainly by a reduction of oxygen in the air. These results show that LiCl is a useful starting material and flux for preparation of lithium manganese oxides.

Effect of heating temperature on composition and morphology of $LiMn_2O_4$ single crystals

The $LiMn_2O_4$ crystals could be obtained at 650, 750, 850 and 950 °C in 4 min. XRD patterns of 650-4m, 750-4m, 850-4m and

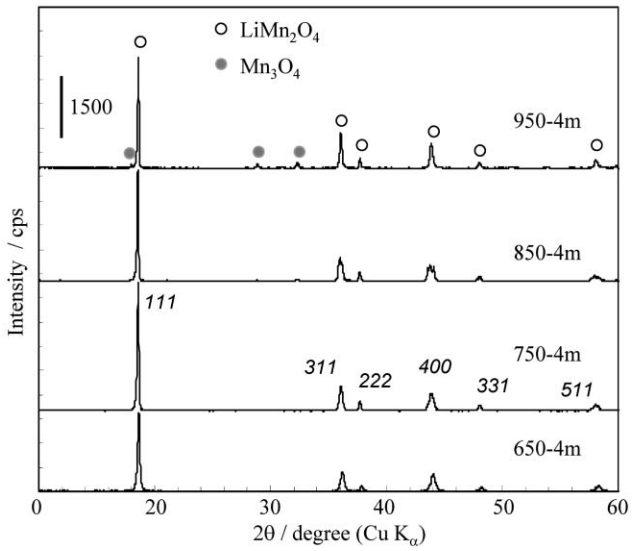

Fig. 2 XRD patterns of 650-4m, 750-4m, 850-4m and 950-4m.

950-4m are given in Fig. 2; 650-4m, 750-4m and 850-4m can be identified as pure $LiMn_2O_4$, while 950-4m consists mainly of $LiMn_2O_4$ but contains a minor amount of Mn_3O_4. The lattice constants of these crystals are shown in Table 1. XRD peaks of these products show broad features, and the peak corresponding to (400) diffraction split is obvious for 850-4m. These results show that $LiMn_2O_4$ crystals are produced rapidly in a $LiCl–Mn(NO_3)_2$ flux system, but the rapid formation results in the formation of crystals with poor crystallinity or distortion.

The SEM images of 650-4m, 750-4m, 850-4m and 950-4m are given in Fig. 3. Plate-like crystals are found in 650-4m, 750-4m and 850-4m, and polyhedral single crystals are found mainly in 950-4m with a small amount of plate-like crystals. The crystallite size increases with increasing temperature. The thickness of the single crystals is less than 0.1 μm for 650-4m and about 0.2 and 0.6 μm for 750-4m and 850-4m, respectively, while the crystals have an average size of about 1.5 μm for 950-4m (Table 1).

The SAED analysis was used to investigate crystallinity and confirm the single crystal feature of the products. The SAED

Table 1 Lattice constant, thickness, analysis result and composition of crystals obtained at 650, 750, 850 and 950 °C in 4 min

Sample	a_0[a] / Å	Thickness/ μm	Analysis result Li : Mn	Analysis result Z_{Mn}[b]	Composition
650-4m	8.18	<0.1	0.58	3.73	$Li_{1.16}Mn_2O_{4.31}$
750-4m	8.22	0.2	0.54	3.56	$Li_{1.08}Mn_2O_{4.10}$
850-4m	8.22	0.6	0.49	3.50	$Li_{0.98}Mn_2O_{3.99}$
950-4m	8.24	1.5[c]	0.45	3.49	$Li_{0.90}Mn_2O_{3.94}$
A650-4m	8.21	<0.1	0.59	3.69	$Li_{1.18}Mn_2O_{4.28}$
A750-4m	8.24	0.2	0.53	3.62	$Li_{1.06}Mn_2O_{4.15}$
A850-4m	8.24	0.6	0.50	3.52	$Li_{1.00}Mn_2O_{4.02}$
A950-4m	8.24	1.5[c]	0.45	3.46	$Li_{0.90}Mn_2O_{3.91}$

[a]Lattice constant. [b]Mean oxidation number of manganese. [c]Average size.

was carried out on three different parts, A, B and C of each crystal, as shown at the top of Fig. 4 for 650-4m, 750-4m and 950-4m. The same SAED patterns were obtained from the three areas for each of the crystals, respectively, and the patterns obtained from area A are given at the bottom of Fig. 4. These patterns can be identified with zone axes of $[\bar{1}\ 2\ \bar{1}]$, $[\bar{1}\ \bar{1}\ 1]$ and $[3\ 1\ \bar{2}]$ for 650-4m, 750-4m and 950-4m, respectively. The results show that the crystals of 650-4m, 750-4m, 850-4m and 950-4m are single crystals. Thus the $LiCl – Mn(NO_3)_2$ system gives fine single crystals of $LiMn_2O_4$ within a short heating time.

The chemical analysis results and composition of 650-4m, 750-4m 850-4m and 950-4m are summarized in Table 1. The chemical formulas in the last column were calculated from the Li : Mn ratio and the mean oxidation numbers of the manganese (Z_{Mn}) in the crystals. Both the Li : Mn ratio and Z_{Mn} decrease with increasing temperature. Crystals with a lithium-rich composition are obtained for 650-4m and 750-4m, an almost theoretical formula of $LiMn_2O_4$ for 850-4m and a lithium-poor composition for 950-4m.

The composition and size of the single crystals depended strongly on the heating temperature. The Mn mean oxidation number as well as Li : Mn molar ratio decrease linearly with increasing temperature. The temperature dependence of the manganese valence shows behavior similar to that of manganese dioxide in air, for which decompositions to

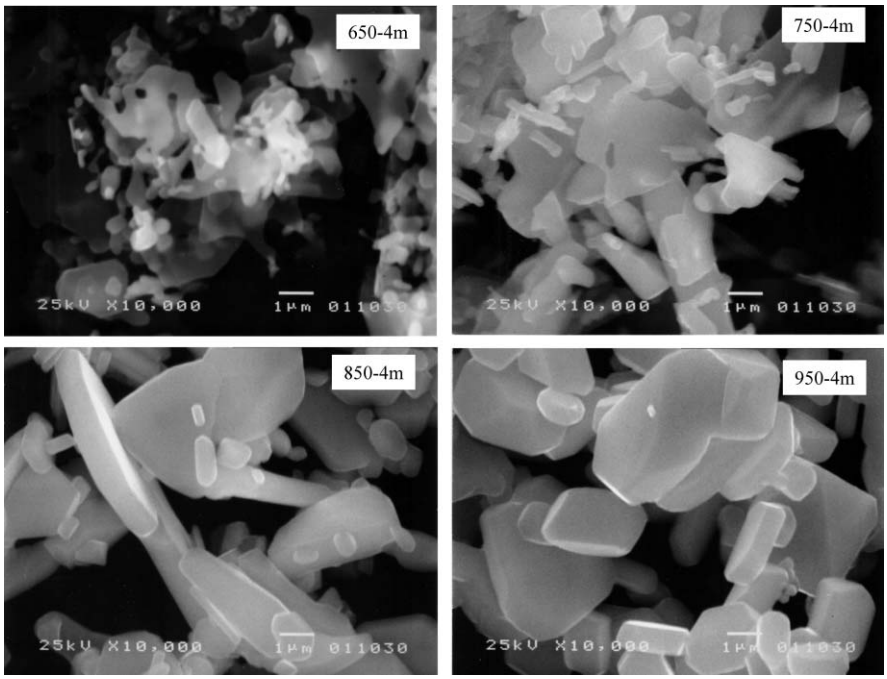

Fig. 3 SEM images of 650-4m, 750-4m, 850-4m and 950-4m.

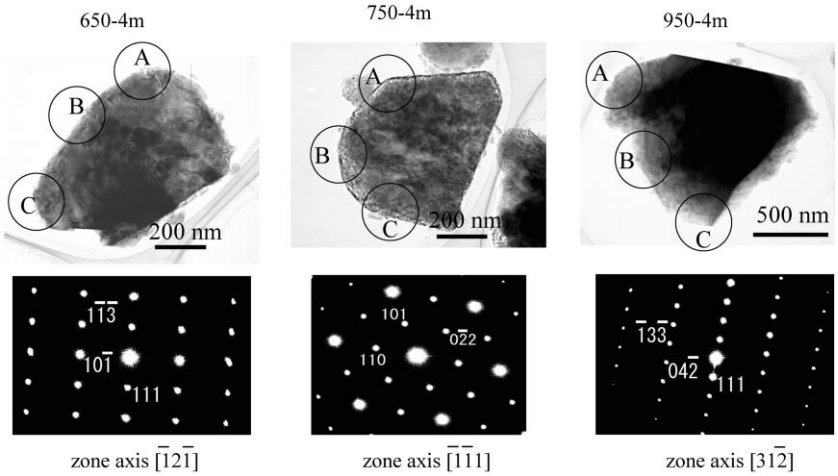

Fig. 4 TEM images and SAED patterns of 650-4m, 750-4m and 950-4m. The electron diffraction was carried out in thin parts marked as circles at the edge of the particles.

Table 2 Lattice constant, thickness, analysis result and composition of crystals obtained at 650 and 750 °C for different times

Sample	a_0[a] / Å	Thickness/ μm	Analysis result		Composition
			Li : Mn	Z_{Mn}[b]	
650-2h	8.23	0.2	0.55	3.68	$Li_{1.10}Mn_2O_{4.23}$
650-8h	8.24	0.3	0.54	3.63	$Li_{1.08}Mn_2O_{4.17}$
650-24h	8.24	0.5	0.52	3.60	$Li_{1.04}Mn_2O_{4.12}$
750-2h	8.24	0.3	0.53	3.57	$Li_{1.06}Mn_2O_{4.10}$
750-8h	8.24	0.7	0.52	3.58	$Li_{1.04}Mn_2O_{4.10}$
750-24h	8.24	2[c]	0.53	3.59	$Li_{1.06}Mn_2O_{4.12}$

[a]Lattice constant. [b]Mean oxidation number of manganese. [c]Average size.

Mn_2O_3 and Mn_3O_4 have been observed at 512 °C and 982 °C respectively.[31,32] This shows that the heating temperature controls mainly the manganese valence in the LiCl melt. The neutral LiCl melt is suitable for preparation of spinel-type lithium manganese oxide. At temperatures lower than 750 °C, oxygen dissolved in the LiCl flux takes part in formation reaction (1) to form lithium-rich crystals. At 950 °C, lithium-poor crystals are formed with a minor amount of Mn_3O_4, probably due to the volatility of Li_2O during heating. The formation reaction (1) of $LiMn_2O_4$ proceeds perfectly at 850 °C.

Changes in morphology, size and composition with heating time

The XRD patterns of the products heated at 650 or 750 °C show the single spinel phase is retained, even when maintained for 24 h at 650 or 750 °C. The diffraction peaks become a little stronger and sharper with heating time at 650 °C. An apparent time dependence of XRD patterns is not observed in samples heat-treated at 750 °C. The results show that the crystal growth by aging is significantly slower than the initial crystallization. The lattice constants are very similar to each other after heating at 650 °C or 750 °C for 2 h or more (Table 2).

SEM images of the plate-like crystal for 650-8h and 650-24h are shown in Fig. 5. The outline of the crystals becomes sharper than for 650-4m. Plate-like crystals similar to 750-4m are also observed for 750-8h. Sample 750-24h consists mainly of polyhedral particles although no significant changes of XRD

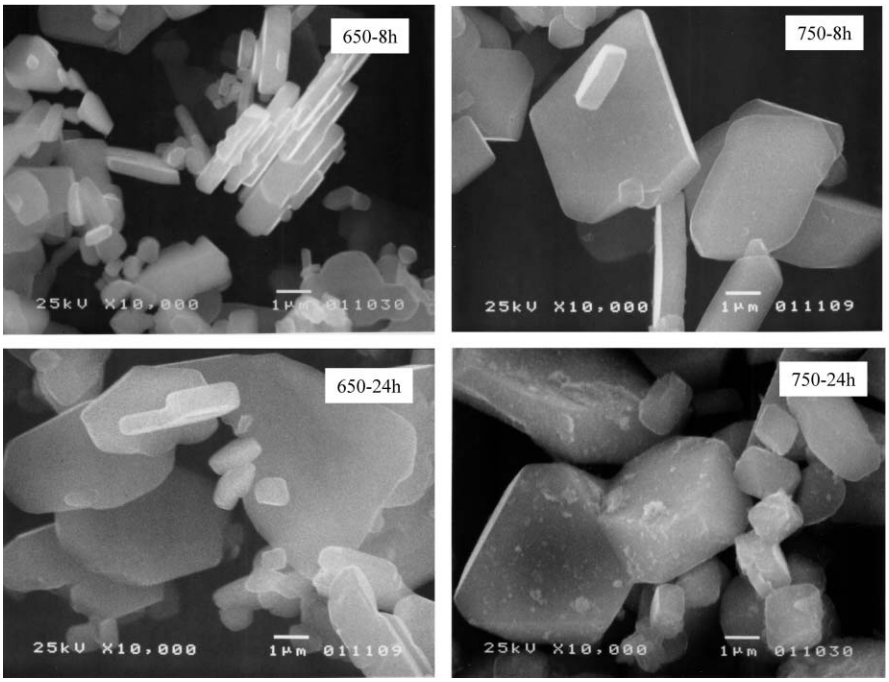

Fig. 5 SEM images of crystals obtained at 650 °C and 750 °C for 8 and 24 h.

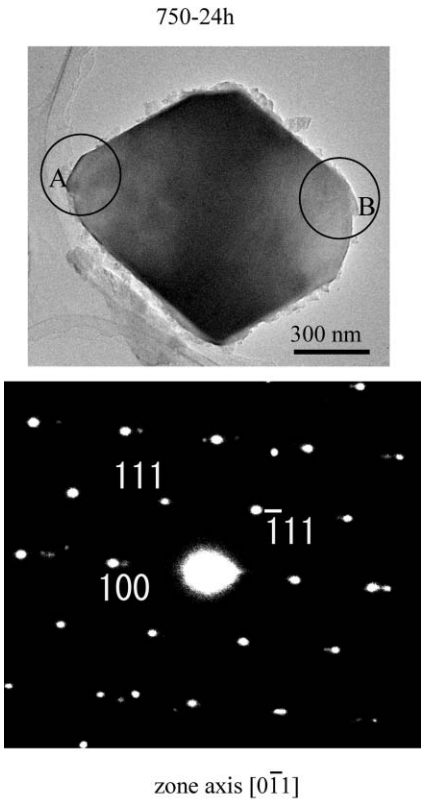

Fig. 6 TEM image and SAED pattern of 750-24h.

patterns were observed between samples 750-8h and 750-24h. Because $LiMn_2O_4$ belongs to a cubic crystal system, it forms hexahedral or octahedral crystals easily. The present results show that plate-like $LiMn_2O_4$ crystals form first and then grow to the polyhedral form in LiCl flux, probably due to Jahn–Teller distortion of the MnO_6 octahedron. The crystal size increases with increasing temperature from 650 to 750 °C as well as with heating time from 4 min to 24 h, as summarized in Tables 1 and 2. The SAED analysis of 750-24h shows that the same SAED pattern was obtained at the two different parts marked with circles in the top of Fig. 6. The SAED pattern obtained from area A is given at the bottom of Fig. 6, and was identified as zone axis [0 $\bar{1}$ 1]. Thus LiCl flux is suitable for the growth of single crystals of spinel-type lithium manganese oxide.

The chemical analysis results are summarized in Table 2 for 650-2h, 650-8h, 650-24h, 750-2h, 750-8h and 750-24h. The Li : Mn ratio and Z_{Mn} decrease slightly with an increase in the heating time from 4 min to 24 h for the crystals obtained at 650 °C. No marked changes in Li : Mn ratio and Z_{Mn} are found for the crystals obtained at 750 °C.

The above results show that the extension of heating time at 650 °C and 750 °C brings about the growth of single crystals, but, however, it has a different effect on the composition. The Li : Mn molar ratio of the crystals decreases and the size increases with heating at 650 °C, whereas the single crystals grow without change in composition at 750 °C.

Effect of post-annealing

The products of 650-4m, 750-4m, 850-4m and 950-4m were post annealed at 750 °C in air to promote their crystallinity. The XRD patterns of A650-4m, A750-4m, A850-4m and A950-4m are given in Fig. 7. The products after the annealing show the spinel structure with the diffraction peaks sharper and higher than those before annealing. The split peak corresponding to (4 0 0) diffraction changes to a sharper peak, indicating that post-annealing promotes the crystallization of the single crystals. The lattice constants of the crystals after annealing

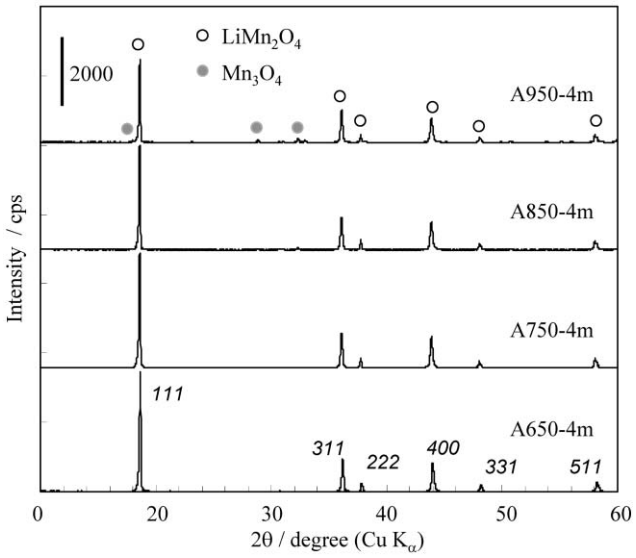

Fig. 7 XRD patterns of A650-4m, A750-4m, A850-4m and A950-4m.

increase slightly, as shown in Table 1. SEM observations did not show any apparent differences in shape or size of the single crystals before and after post-annealing. Chemical analysis results and composition of A650-4m, A750-4m A850-4m and A950-4m are summarized in Table 1. There are small changes in the Li : Mn ratio and Z_{Mn} for the crystals before and after post-annealing. The single crystals with a lithium-rich composition are maintained for A650-4m and A750-4m, and a theoretical formula of $LiMn_2O_4$ for A850-4m and a lithium-poor composition for A950-4m after post-annealing.

The crystals after annealing are also single crystals. The post-annealing promotes the crystallinity of the single crystals without apparent changes in their composition, shape or size. The post-annealing process is useful for obtaining fine single crystals with a well-ordered structure, because although fine single crystals can be obtained in a short time, they may have poor crystallinity or a distorted structure.

Electrochemical measurement

The electrochemical studies were carried out using A650-4m as a cathode material. For comparison, a charge/discharge test of a commercial product, $Li_{1.33}Mn_2O_{4.267}$ (purchased from Nikki Chemical Co., Ltd.) was also carried out. The latter product was prepared by reacting the electrolytic manganese dioxide (EMD) and lithium salt after aqueous mixing. The particle is a polycrystal with an average size of about 11 μm. The two samples have similar lithium-rich compositions, but differ in particle morphology.

The charge/discharge curves of A650-4m and commercial $Li_{1.33}Mn_2O_{4.267}$ are given in Fig. 8A. The A650-4m shows a one step charge/discharge curve similar to that of commercial $Li_{1.33}Mn_2O_{4.267}$. Suppression of the two-step charge/discharge characteristic indicates lithium occupation of the 16d site, which suppresses the formation of $Li_{0.5}Mn_2O_4$ during the lithiation/delithiation process of the spinel, as was reported in the studies of lithium-rich polycrystal.[33] The first discharge capacity of A650-4m is 112 mAh g^{-1}, slightly higher than that of commercial $Li_{1.33}Mn_2O_{4.267}$ (105 mAh g^{-1}). The 15th discharge capacity is the same (102 mAh g^{-1}) for both the A650-4m and commercial $Li_{1.33}Mn_2O_{4.267}$. The coulombic efficiency reaches 95% at the first cycle and as high as 99.4% from the second cycle for A650-4m. This shows that the cathode of a lithium-rich single crystal has one-step voltage curves, high discharge capacity and excellent cycle features similar to those of the commercial one. The good crystallization and continuous lattice structure of the single crystal

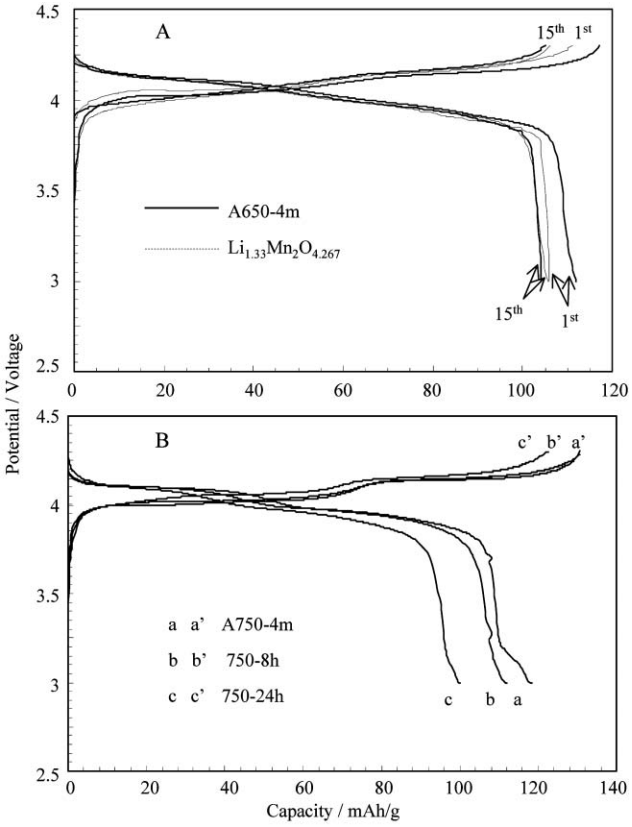

Fig. 8 Charge/discharge curves for: A, A650-4m and commercial $Li_{1.33}Mn_2O_{4.267}$; and B, A750-4m, 750-8h and 750-24h.

and lithium-rich composition probably play an important part in improvement of cycle features.

The effect of crystal size on the charge/discharge feature was studied using A750-4m, 750-8h and 750-24h. These samples have slightly lithium-rich compositions of $Li_{1.06}Mn_2O_{4.15}$, $Li_{1.04}Mn_2O_{4.10}$ and $Li_{1.06}Mn_2O_{4.12}$, respectively, but differ in size as shown in Tables 1 and 2. These single crystals show clear two-step charge/discharge curves as shown in Fig. 8B, similar to previous studies for single spinel crystal and polycrystal.[34,35] The two-step character was explained by formation of a semi-stable phase of $Li_{0.5}Mn_2O_4$ during the lithiation/delithiation process.[36] The capacity fade of these crystals runs parallel to an increase in the cycle number from about the fourth cycle, as shown in Fig. 9. The results show that the increases in size of the single crystals do not accelerate the capacity fade after the initial few cycles.

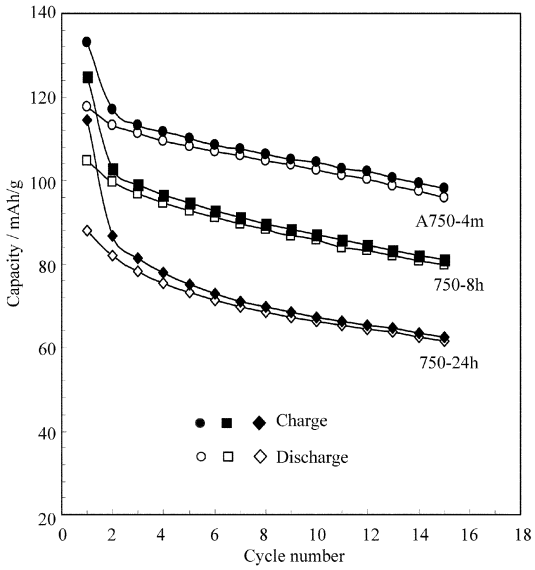

Fig. 9 Capacity fade of A750-4m, 750-8h and 750-24h with cycle number.

The discharge curves show that the first step corresponding to the reaction from MnO_2 to $Li_{0.5}Mn_2O_4$ (at 4.06 V) is more crystal-size dependent than the second step corresponding to the reaction from $Li_{0.5}Mn_2O_4$ to $LiMn_2O_4$. The capacity in the first step decreases significantly from 46 to 31 mAh g^{-1} with an increase in the crystal size. It is well known that the former reaction progresses by phase transition, while the latter by one-phase solid insertion reaction.[36] The Li^+ insertion reaction in the first step may be suppressed by the steric effect due to the difference in lattice parameter between the two phases. In addition, the diffusivity of Li^+ in a single crystal is known to be markedly lower than that in a polycrystalline solid.[6,7] These results suggest that the Li^+ diffusion during the charge/discharge reaction does not progress all over the crystal, but progresses up to a limited depth of the crystal. The effective shell, which is active for the electrochemical reaction, may be formed in the crystal, with the thickness depending on the electric current. The idea of an effective shell explains well the difference in the charge/discharge characteristics observed for samples A750-4m, 750-8h, and 750-24h, since the volume of the effective shell at a constant electric current decreases with increasing crystal size, due to the decrease in specific surface area.

Conclusions

The LiCl–$Mn(NO_3)_2$ flux method is useful for the preparation of fine spinel-type lithium manganese oxide single crystals. The composition, shape and size of the single crystals can be controlled by adjusting heating temperature and time. Fine lithium-rich spinel single crystals with a plate shape less than 0.1 mm in thickness were obtained by heating at 650 °C for 4 min. The crystals after post-annealing show a one-step charge/discharge behavior with a high capacity of 112 mAh g^{-1} at the first discharge cycle and an excellent cycle feature. Single crystals with the same composition but of different sizes were obtained by heating at 750 °C for different times. These crystals show two-step charge/discharge curves. The increase in the crystal size results in a decrease of capacity at the first cycle, but does not accelerate the capacity fade after the initial few cycles.

References

1 A. Yamada, K. Miura, K. Hinokuma and M. Tanaka, *J. Electrochem. Soc.*, 1995, **142**, 2149.
2 T. Ohzuku, J. Kato, K. Sawai and T. Hirai, *J. Electrochem. Soc.*, 1991, **138**, 2556.
3 M. M. Thackeray, *Prog. Batteries Battery Mater.*, 1995, **14**, 1.
4 K. Dokko, M. Nishizawa, M. Mohamedi, M. Umeda, I. Uchida, J. Akimoto, Y. Takahashi, Y. Gotoh and S. Mizuta, *Electrochem. Solid-State Lett.*, 2001, **4**, A151.
5 H. Kanoh, Q. Feng, Y. Miyai and K. Ooi, *J. Electrochem. Soc.*, 1995, **142**, 702.
6 D. Guyomard and J. Tarascon, *J. Electrochem. Soc.*, 1992, **139**, 937.
7 G. Pistoia, G. Wang and C. Wang, *Solid State Ionics*, 1992, **58**, 285.
8 X. M. Shen and A. Clearfield, *J. Solid State Chem.*, 1986, **64**, 270.
9 K. Ooi, Y. Miyai and Y. Kato, *Solvent Extr. Ion Exch.*, 1987, **5**, 561.
10 M. M. Thackeray, W. I. F. David, P. G. Bruce and J. B. Goodenough, *Mater. Res. Bull.*, 1983, **18**, 461.
11 D. G. Wickham and W. J. Croft, *J. Phys. Chem. Solids*, 1958, **7**, 351.
12 Q. Feng, H. Kanoh, Y. Miyai and K. Ooi, *Chem. Mater.*, 1995, **7**, 1226.
13 Y. Wang, S. Nishiuchi, T. Kuroki, N. Yamasaki and S. Takikawa, in *3rd Int. Conf. Solvothermal Reactions*, Bordeaux, France, July 19, 1999.

14 S. Bach, M. Henry, N. Baffier and J. Livage, *J. Solid State Chem*, 1990, **88**, 325.
15 B. Ammundsen, D. J. Jones, J. Roziere and G. R. Burns, *Chem. Mater.*, 1997, **9**, 3236.
16 A. R. Naghash and J. Y. Lee, *Lithium Batteries*, 2000, 364.
17 W. Liu, G. C. Farrington, F. Chaput and B. Dunn, *J. Electrochem. Soc.*, 1996, **143**, 879.
18 W. Tang, H. Kanoh and K. Ooi, *J. Solid State Chem.*, 1999, **142**, 19.
19 W. Tang, H. Kanoh, X. Yang and K. Ooi, *Chem. Mater.*, 2000, **12**, 3271.
20 W. Tang, H. Kanoh and K. Ooi, *Chem. Lett.*, 2000, 216.
21 W. Tang, X. Yang, H. Kanoh and K. Ooi, *Chem. Lett.*, 2001, 524.
22 X. Yang, W. Tang, H. Kanoh and K. Ooi, *J. Mater. Chem.*, 1999, **9**, 2683.
23 X. Yang, H. Kanoh, W. Tang and K. Ooi, *J. Mater. Chem.*, 2000, **10**, 1903.
24 X. Yang, H. Kanoh, W. Tang, Z. Liu and K. Ooi, *Chem. Lett.*, 2000, 1192.
25 X. Yang, W. Tang, H. Kanoh and K. Ooi, *J. Mater. Chem.*, 2002, **12** , 489.
26 Japan Industrial Standard (JIS) M8233, 1969.
27 T. J. W. de Bruijn, W. A. de Jong and P. J. van den Berg, *Thermochim. Acta*, 1981, **45**, 265.
28 T. J. W. de Bruijn, G. M. J. de Ruiter, W. A. de Jong and P. J. van den Berg, *Thermochim. Acta*, 1981, **45**, 279.
29 J. Pelovski, O. Matova and St. Shoumkov, *Thermochim. Acta*, 1992, **196**, 503.
30 J. Akimoto, Y. Takahashi, Y. Gotoh and S. Mizuta, *Chem. Mater.*, 2000, **12**, 3246.
31 J. P. Brenet, J. P. Gabano and M. Seighneurin, in *Proc. IUPAC Symp., Paris, 1957*, Sades, Paris, 1958, p. 69.
32 P. Strobel, H. G. Wiedemann and R. Giovanoli, *Calorim. Anal. Therm.*, 1982, **13**, 71.
33 Y. J. Lee, R. Wang, S. Mukerjee, J. McBreen and C. P. Grey, *J. Electrochem. Soc.*, 2000, **147**, 803.
34 H. Bjork, T. Gustafsson and J. O. Thomas, *Electrochem. Commun.*, 2001, **3**, 187.
35 J. M. Tarascon, E. Wang, F. K. Shokoohi, W. R. McKinnon and S. Colson, *J. Electrochem. Soc.*, 1991, **138**, 2859.
36 K. Ooi, Y. Miyai, S. Katoh, H. Maeda and M. Abe, *Langmuir*, 1989, **5**, 150.